一般社団法人　電子情報通信学会
THE INSTITUTE OF ELECTRONICS,
INFORMATION AND COMMUNICATION ENGINEERS

信学技報
IEICE Technical Report
A・P2022-72(2022-09)

Double convex lens for marine retro-reflector application

Derek GRAY †　,　John THORNTON ‡　and Julien Le KERNEC †

† James Watt School of Engineering,　University of Glasgow,　Glasgow,　UK

‡ Antennas Research Ltd.,　York,　UK

E-mail:　john@thorntonj.myzen.co.uk,　(Derek.Gray, Julien.LeKernec) @glasgow.ac.uk

Abstract　Polyethylene 4 free space wavelength radius spherical lenses fitted with 140° spherical metallic cap were found to satisfy the ISO8729 RCS requirement for use on buoys and small fishing and leisure boats.　Double convex polyethylene lenses were trialed as a reduced mass alternative to the spherical lenses.　An initial prototype fitted with custom reflector back plate shaped to follow the lens focal arc satisfied ISO8729 across a 60° arc.　The double convex lens had 25% the weight of a spherical lens.

Key words　radar target enhancer,　lens antenna

1. Introduction

Arrays of 3 Luneburg lenses fitted with 140° reflective caps are used on marine on marine safety buoys marking port entrances,　channels and reefs.　Another marine safety application entails increasing the radar cross-section (RCS) of small vessels under 150 gross tonnage which are poor reflectors of radar signals which is a contributor to the average of 780 vessels damaged in collisions per year in Japanese territorial waters [1].　Despite 3 Luneburg lens arrays been the only product in the market that satisfies ISO8729 at 9.41GHz,　the high cost is an impediment to widespread adoption [2].　As the array element Luneburg lens radius has a radius around $4\lambda_0$ replacement by a simple homogeneous spherical lenses is possible,　as for normal antenna applications.　This has been confirmed by some experimental measurements and a follow-up simulation study [3].　Inserting an airgap between the spherical lens and the reflective cap allowed the use of lower specific gravity plastics such as high density polyethylene (HDPE) and cross-linked polystyrene (CPS),　which were taken to be lossless in simulation [4].

The relative permittivity (ε_r') and loss tangent ($tan\delta$) of a selection of commercially available plastics has been published [5] and were summarized in Table 1.　The measurements were made across -150 to 100°C, encompassing the working temperature range of marine vessels.

TABLE 1:　25°C plastic properties,　from [5, 6].

plastic	ε_r'	tanδ
FEP	2.025	$4e^{-3}$
PTFE	2.03	$6e^{-3}$
polymethyl pentene (TPX)	2.1	$8e^{-4}$
polypropylene (PP)	2.26	$8e^{-5}$
polyethylene (HDPE)	2.37	$1.5e^{-4}$
polystyrene (CPS)	2.535	$4.8e^{-4}$
acrylic (PMMA)	2.61	$8e^{-3}$
polycarbonate (PC)	2.77	$5e^{-4}$
ABS	2.79	$7.5e^{-3}$
nylon	3.03	$8e^{-3}$

Having a database of measured ε_r' and tanδ enables assessment of the limitations imposed by those properties on the performance of homogeneous spherical lens antennas and the derivative spherical lens reflectors.　Such a study of losses is presented followed by initial results from an alternative non-spherical lens reflector.

As with prior work,　all results presented here are from 12GHz scaled models due to available legacy equipment.

2. Losses in a spherical lens antennas

The empirical equations of [7] enable building a simple "theoretical" loss model of aperture restriction imposed by ε_r' and losses that will occur within the spherical lens due to *tanδ*. This model assumes that the homogeneous spherical lens is a purely optical device and has no non-optical effects. The behavior of the feed is not accounted for, nor are the surface reflections.

Combining equations (3) and (4) of [7] gave the spherical lens radius reduction caused by the complete internal reflection limit at the lens aperture edge due to the lens ε_r. The aperture restriction matched the RCS roll-off seen in FEKO™ simulations [3, 4]. This reduced radius was used for a theoretical circular aperture Gain calculation from which the dielectric losses calculated using equation 6 of [7] were subtracted. An aperture efficiency of 50% was used for the Gain calculation.

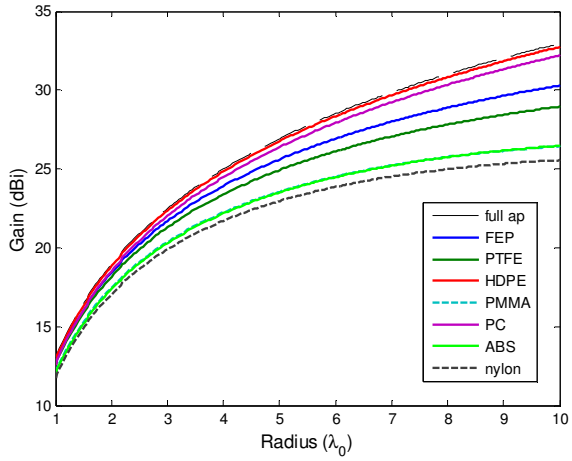

Figure 1: Predicted spherical lens antenna Gain variation with radius for plastics from Table 1 at 25°C.

The plastics in Table 1 were used in the spherical lens loss model and compared to lossless full radius circular apertures having 50% aperture efficiency, Figure 1. The 4 plastics TPX, PP, HDPE and CPS were indistinguishable and suffered very little loss compared to full circular aperture due to the combined effects of lower ε_r' and low *tanδ*. For brevity only the HDPE trace was presented in Figure 1. PC suffered slightly higher losses as had a higher ε_r' which reduced the aperture radius. A balance between ε_r' and *tanδ* caused ABS and PMMA to give identical Gain characteristics. The worst results were from nylon which had both high ε_r' and high *tanδ*. Both FEP and PTFE had low ε_r' and thus almost no aperture radius reduction but suffered high dielectric losses. Thus lenses built from these materials will have high self-generated noise figures, and should be avoided.

Flat circular aluminium plates have been used as RCS calibration standards in prior RCS work as those were easy to manufacture and gave significantly higher returns than metallic spheres. Luneburg lens reflectors have historically been compared to circular plates of the same radius. The circular plate RCS equation of [8] was used as the baseline for a loss assessment model for the homogeneous spherical lens reflectors in place of the circular aperture Gain equation used in the antenna loss model above. As the radio waves impinging on the spherical lens traverse the lens, reflect off the 140° metallic spherical cap and then travel back through the lens to be re-radiated in the direction of the illuminator, the dielectric losses calculated using equation 6 of [7] must be subtracted twice. Thus a spherical lens reflector will suffer doubly from any dielectric loss and quadruply from internal noise. For ease of comparison to prior work, the modified ISO8729 6.64dBm² RCS line was marked on Figure 2.

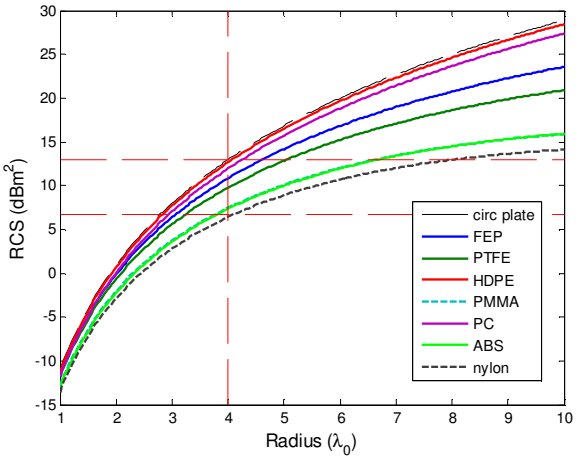

Figure 2: Predicted spherical lens reflector RCS variation with radius for plastics from Table 1 at 25°C.

As for the antenna case, TPX, PP, HDPE and CPS were indistinguishable and suffered less loss than PC,

Figure 2. For this group of low loss plastics, the loss compared to the ideal circular plate ranged from 0.8dB for a lens radius of $1\lambda_0$ to 1.5dB for a radius of $10\lambda_0$. The loss was 1dB for a radius of $4\lambda_0$, which was the radius previously judged to satisfy ISO8729. As for the antenna case above, ABS and PMMA were close to identical.

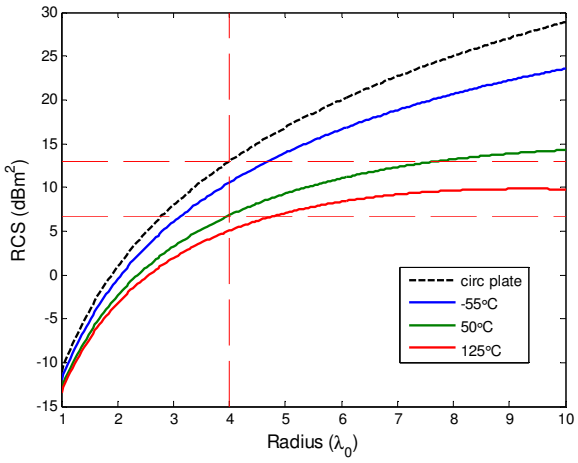

Figure 3: Temperature effects on RCS of acrylic (PMMA) spherical lens reflector.

Despite the high losses, the RCS of the $4\lambda_0$ radius acrylic (PMMA) lens did exceed the modified ISO8729 specification by 0.8dB. This is of particular interest as large radius spheres are already manufactured at scale and freely available at low cost. Additionally, this plastic has been used as a high wind loading exterior window for more than 80 years and thus could be used without a weather proof radome, giving an advantage in reduced number of parts. Measurements of ε_r' and $tan\delta$ were made at the bottom of the Mil. Std. temperature range, and the top can be found by extrapolation of Figure 10 of [5]. The peak value $tan\delta = 9x10^{-3}$ occurred at 50°C with $\varepsilon_r' = 2.62$. For $4\lambda_0$ radius, the model predicted that the RCS would be 1.6dB below ISO8729 at -125°C, Figure 3. Thus a long period of heating due to direct sunlight exposure will cause an acrylic homogeneous lens to fail ISO8729. There will be 5.5dB RCS variation across Mil. Std. temperature range. In contrast, CPS had less than 0.1dB RCS variation across the same temperature range. Thus from this superficial analysis using simple empirical equations, there is a considerable advantage to using CPS or HDPE stemming from the low dielectric loss and the minimal aperture restriction from ε_r'. This fits well with the better performance from these same plastics in full-wave, but lossless, simulations in prior work which concentrated with focusing on the spherical cap reflector [4].

It was envisioned that the homogeneous spherical lenses would be used in a 3 element circular array attached to a boat mast identical to what is used for Luneburg lenses. As each $4\lambda_0$ radius CPS or HDPE lens will weigh 4kg the bracket holding the lenses in place and attaching to the boat mast will have to be moulded from 6063 Aluminium alloy. Reducing the mass of the lenses would facilitate suspending the parts inside a moulded styrofoam armature reducing manufacturing costs and easing installation. Two obvious means of lens mass reduction are to change from natural plastics to a conductive wire effective media or change the type of lens used. The former is trivial. An aplanatic lens was trialed for the latter.

3. Double convex lens reflectors

Medium to high Gain beam scanning using aplanatic lenses was first tried nearly 80 years ago [8]. The lens was close to planoconvex where the planar lower surface had a small indentation. A major advance in the design process was made about 55 years ago when the first computer Fortran code was written thus avoiding the series of laborious manual calculations [9]. A double convex lens was given in Figure 10.37 of [10] as an alternative to the traditional quasi-planoconvex with no background explanation, no design worked example and no typical performance results. A scan of the illustration was traced using CorelDRAW™ to get the lower and upper surface shapes which were used as a guides to design 2 HDPE plastic lenses using a Matlab™ transcription of the Fortran code from [9], Figure 4. The first lens had a radius of 100mm ($4\lambda_0$), while the second had a radius of

141mm and could be cut down to a 200mm sided square. The apex position for both lenses was z=200mm, making *f*/D=1 for both. The R=100mm lens would weigh 0.98kg and the R=141mm lens 2.6kg.

Both were simulated in FEKO™ as rotationally symmetric circular lenses with X-axis aligned axes illuminated by a horizontal linearly polarized plane wave, and the focal arc was traced for incident angles from 0° to 45°, Figure 4. Neither focal arc passed through the design focal point (0, 0).

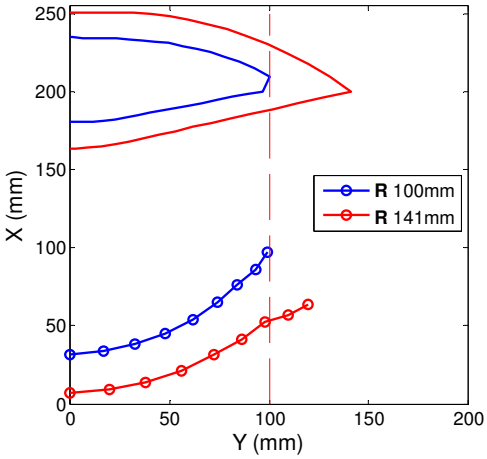

Figure 4: Double convex HDPE lenses with plane wave response focal arc for illumination angles from 0° to 45°; both lenses apex was z=200mm, from FEKO™.

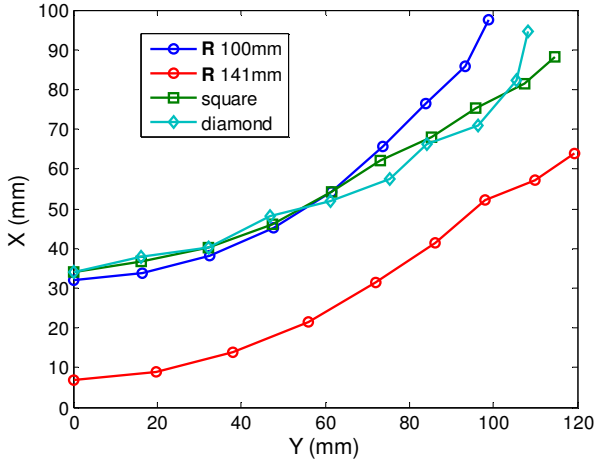

Figure 5: Near field peak focal arcs of circular lenses and R=141mm lens cut down to 200mm sided square; same scale as Figure 4, from FEKO™.

The 141mm radius lens was cut down to a 200mm sided square, and the series of plane wave illumination simulations was rerun in FEKO™. This square lens was run as a "square" with sides parallel to the Y and Z-axes, and rotated 45° about the X-axis in a "diamond" orientation. The focal arc of both square lens orientations were close to the circular R=100mm lens, Figure 5. The causes of focal arc change from removing the edges of this type of lens will be investigated with ray tracing software in the future.

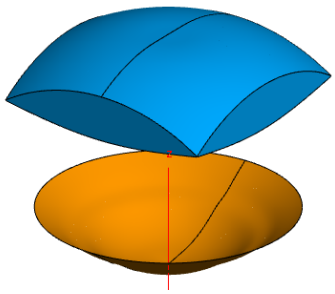

Figure 6: CAD of R=141mm lens cut down to a 200mm sided square; from FEKO™.

The traced focal arc of the square lens was rotated 360° to form a thin conductive bowl shaped reflector, Figure 6. This lens reflector system was rotated from 0° to 45° about the lens apex x=200mm and the monostatic RCS was noted. The RCS was above the modified ISO 8729 specification to ϕ=35°, Figure 7. This novel lens reflector gave sufficient RCS across a 70° span of the horizontal plane so a circular array of 5 lenses would satisfy ISO 8729, Figure 8.

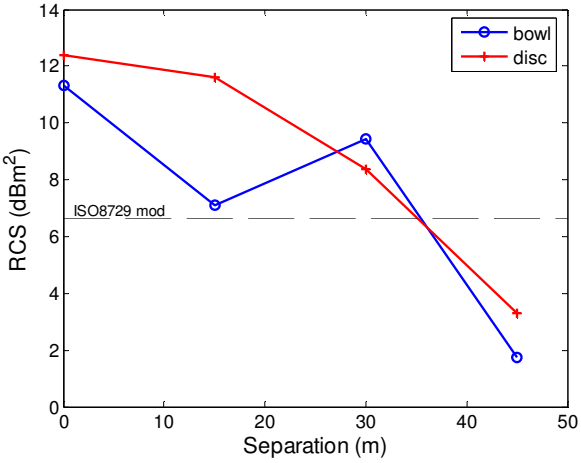

Figure 7: Simulated monostatic RCS of square lens with focal arc reflector bowl or disc for example rotated horizontal plane angles; from FEKO™.

The ϕ=15° monostatic RCS was inconsistent with the ϕ=0° and ϕ=30° returns, Figure 7. The horizontal plane bistatic RCS patterns were examined, Figures 9 to 12. The ϕ=0° and ϕ=30° patterns had well defined main lobes directed back at the illuminator, thus having relatively little power sent in other directions as occurs with corner

reflector arrays which is a potential source of interference [4]. The ϕ=15° pattern still had a main lobe but the beamwidth had doubled causing the loss of directivity. At ϕ=45° the pattern shape had entirely broken down, Figure 12.

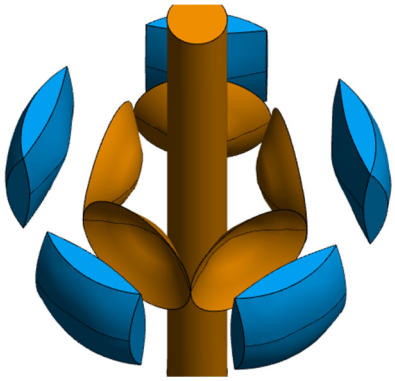

Figure 8: CAD of 5 square lens around a boat mast to provide full horizontal coverage; from FEKO™.

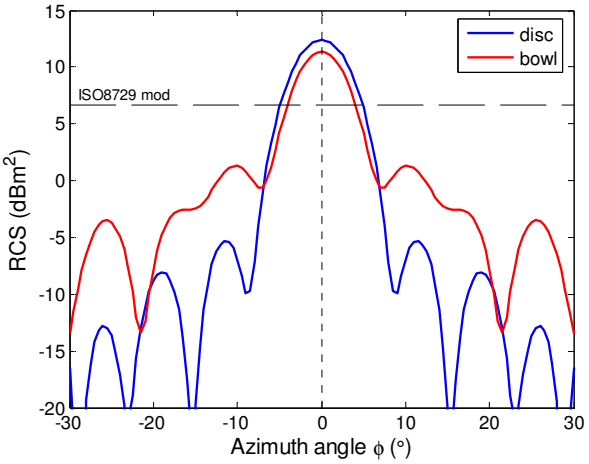

Figure 9: Simulated 0° scan bistatic RCS of square lens with focal arc reflector bowl or disc; from FEKO™.

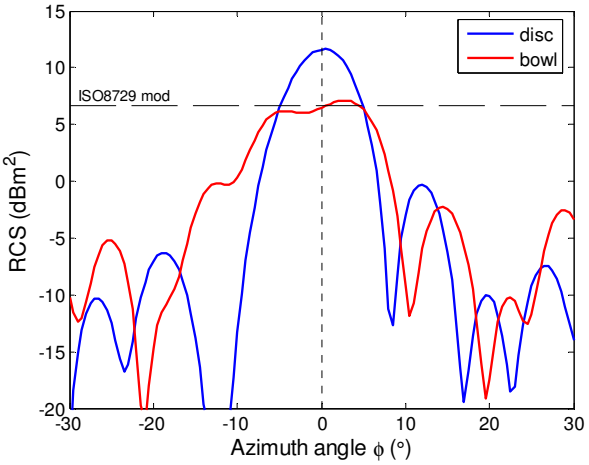

Figure 10: Simulated 15° scan bistatic RCS of square lens with focal arc reflector bowl or disc; from FEKO™.

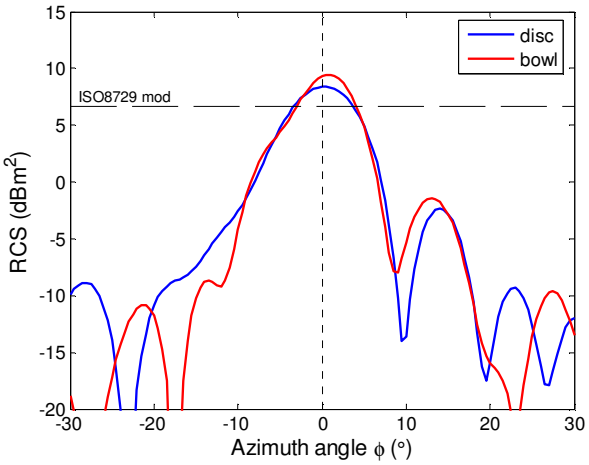

Figure 11: Simulated 30° scan bistatic RCS of square lens with focal arc reflector bowl or disc; from FEKO™.

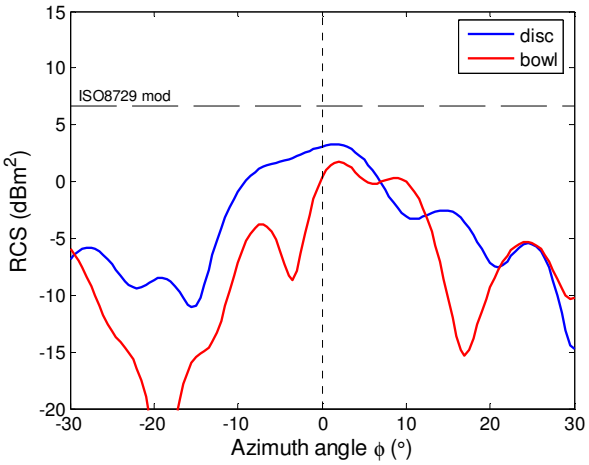

Figure 12: Simulated 45° scan bistatic RCS of square lens with focal arc reflector bowl or disc; from FEKO™.

4. Square lens with disc reflector

As an initial attempt to optimize the bowl reflector, the position of a flat 30mm radius disc was optimized for highest RCS across ϕ=0° to ϕ=45°, Figures 13 and 14. The square lens was rotated about the apex at x=200mm.

The arc of optimal disc position was further away from the lens and roughly parallel to the focal arc, Figure 15. The bistatic RCS patterns were better than those with the bowl, Figures 9 to 12, giving better monostatic performance, Figure 7.

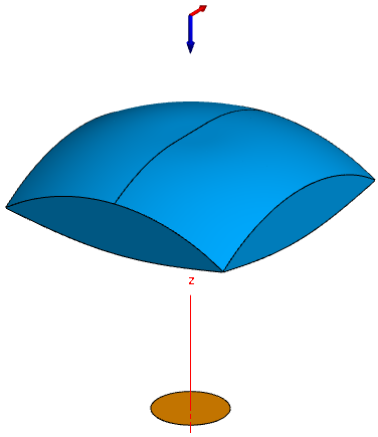

Figure 13: CAD of square lens with circular reflecting disc for ϕ=0° incidence; from FEKO™.

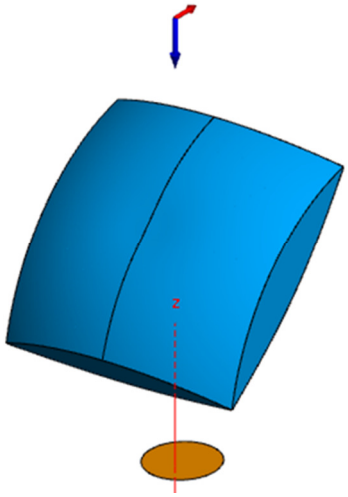

Figure 14: CAD of square lens with circular reflecting disc for ϕ=0° incidence; from FEKO™.

5. Conclusions

A superficial study of the effect of aperture radius reduction from measured ε_r' and dielectric loss $tan\delta$ using some empirical equations showed that 2 widely available plastics with ε_r=2.3 and ε_r=2.54 gave the lowest losses as 100mm ($4\lambda_0$) radius spherical lens radar reflectors. This finding adds to the case for using those 2 plastics having previously found from full-wave simulation studies that those gave the best focus control. A ε_r=2.3 double convex lens reflector was trialed as a weight reduced alternative to the spherical lens reflectors. The weight was reduced from 4kg to 2kg but the ISO 8729 compliant range was reduced from 120° to 70°.

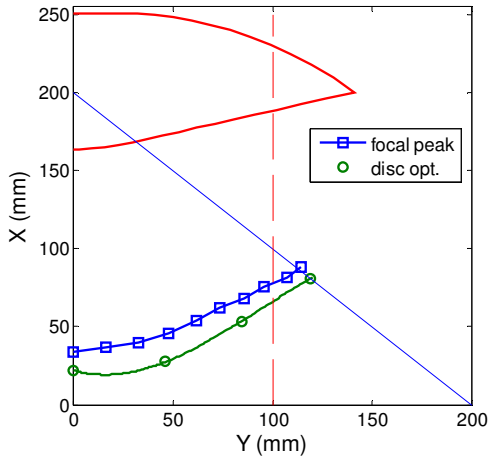

Figure 15: Comparison of square clipped lens focal arc with optimal disk position; from FEKO™.

Acknowledgement

The authors wish to thank Dr. M. Ide of MOL Marine & Engineering Co.,Ltd. for her advice, encouragement and enthusiasm.

8. References

[1] H. Heibatake, S. Hayashi & M. Ide, "A basic study on enhancement of electrical visualization for small boat," *Asia Navigation Conf. 2008*, Shanghai, Nov. 2008.

[2] S. Luke, "Performance investigation of marine radar reflectors on the market," *QinetiQ CR0704527*, Mar. 2007.

[3] D. Gray, "Homogeneous spherical lens for marine retro-reflector application," *IEICE Tech. Rep.*, Takamatsu, vol. 119, no. 379, AP2019-178, pp. 153-158, Jan. 2020.

[4] D. Gray, J. Le Kernec & J. Thornton, "Homogeneous spherical lens for marine retro-reflector application, part 3," *IEICE Tech. Rep.*, Kobe Port Oasis, vol. 122, no. 34, AP2022-21, May 2022.

[5] B. Riddle, J. Baker-Jarvis & J. Krupka, "Complex permittivity measurements of common plastics over variable temperature," *IEEE Trans. Microw. Theory Tech.*, vol. 51, pp. 727–733, 2003.

[6] *Polymethyl Pentene (PMP) TPX*, Mitsui Chemicals, Inc., Minato-ku, Tokyo, Japan, Revision Sept. 2011.

[7] T.C. Cheston & E.J. Luoma, "Constant-k lenses," *APL Technical Digest*, vol. 2, no. 4, pp. 8-11, March-April 1963.

[8] H. Gent, "Theoretical design and performance of a dielectric lens for wide-angle scanning," *T.R.E. Tech. Note 105*, 1951.

[9] J.F. Kauffman, "Microwave lenses for amplitude and phase transformation," Ph.D. dissertation, Dept. Elect. Comp. Eng., North Carolina State University, Raleigh, 1970.

[10] J.J. Lee, "Lens antennas," in *Handbook of rf/microwave components and eng.*, K. Chang, Ed., Hoboken: John Wiley & Sons, 2003, sec. 10.2, p. 595.